

The crystal chemistry of duftite, $\text{PbCuAsO}_4(\text{OH})$ and the β -duftite problem

KHARISUN*, MAX R. TAYLOR, D. J. M BEVAN

Department of Chemistry, The Flinders University of South Australia, GPO Box 2100 Adelaide, S. A. 5001, Australia

AND

ALLAN PRING

Department of Mineralogy, South Australian Museum, North Terrace, S. A. 5000, Australia

ABSTRACT

Duftite, $\text{PbCu}(\text{AsO}_4)(\text{OH})$ is orthorhombic, space group $P2_12_12_1$ with $a = 7.768(1)$, $b = 9.211(1)$, $c = 5.999(1)$ Å, $Z = 4$; the structure has been refined to $R = 4.6\%$ and $R_w = 6.5\%$ using 640 observed reflections [$F > 2\sigma(F)$]. The structure consists of chains of edge-sharing CuO_6 'octahedra', parallel to c ; which are linked via AsO_4 tetrahedra and Pb atoms in distorted square antiprismatic co-ordination to form a three dimensional network. The CuO_6 'octahedra' show Jahn-Teller distortion with the elongation running approximately along $\langle 627 \rangle$. The hydrogen bonding network in the structure was characterized using bond valence calculations. ' β -duftite' is an intermediate in the duftite–conichalcite series, which has a modulated structure based on the intergrowth of the two structures in domains of approximately 50 Å. The origin of the modulation is thought to be associated with displacements in the oxygen lattice and is related to the orientation of the Jahn-Teller distortion of CuO_6 'octahedra'. Approximately half of the strips show an elongation parallel to $\langle 627 \rangle$ while the other strips are elongated parallel to $[010]$. This ordering results in an increase in the b cell repeat compared to duftite and conichalcite.

KEYWORDS: duftite, conichalcite, crystal structure, crystal chemistry, modulated structure.

Introduction

DUFTITE, a lead cupric hydroxy arsenate, $\text{PbCu}(\text{AsO}_4)(\text{OH})$ was originally described by Pufahl (1920) from the Tsumeb mine, in what is now Namibia. The mineral occurs in some abundance with other lead and copper arsenates, calcite and azurite throughout the oxidized zones of this complex deposit (Keller, 1977). Richmond (1940) determined the unit cell parameters for duftite as $a_0 = 7.50$ $b_0 = 9.12$ $c_0 = 5.90$ kX but was unable to assign the space group; Pufahl (1920)

had earlier tentatively proposed the point group 222, on the basis of morphological observations. Guillemin (1956) identified two distinct polymorphs of duftite on specimens from Tsumeb, which he denoted as ' α -duftite' with the unit cell $a = 7.81$, $b = 9.19$, $c = 6.08$ Å and ' β -duftite' which has the slightly different unit cell $a = 7.49$, $b = 9.36$, $c = 5.91$ Å. He proposed that ' α -duftite' is isomorphous with descloizite, $\text{PbZn}(\text{VO}_4)(\text{OH})$, and has the space group $Pnam$ while ' β -duftite' is isomorphous with conichalcite, $\text{CaCu}(\text{AsO}_4)(\text{OH})$, which has the space group $P2_12_12_1$. His chemical analyses suggested that the α -form is almost pure $\text{PbCu}(\text{AsO}_4)(\text{OH})$ while the β -form has approximately 20% Ca substituted for Pb. While Guillemin (1956) was able to prepare the α -form synthetically his attempts to prepare the β -form were unsuccessful. The

* Permanent address: Fakultas Pertanian, Universitas Djenderal Soedirman, P.O. Box 125, Purwokerto 53123, Jawa-Tengah, Indonesia

duftites are members of the adelite group which includes, adelite, $\text{CaMn}(\text{AsO}_4)(\text{OH})$, conichalcite, $\text{CaCu}(\text{AsO}_4)(\text{OH})$, austinite, $\text{CaZn}(\text{AsO}_4)(\text{OH})$, and gabrielsonite, $\text{PbFe}(\text{AsO}_4)(\text{OH})$, and extensive solid solution fields have been reported between members of this series (Radcliffe and Simmons, 1971; Jambor *et al.*, 1980; Taggart and Foord, 1980). Jambor *et al.* (1980) examined a series of calcian duftite and plumbian conichalcite specimens from Tsumeb and concluded that complete solid solution exists between the Ca and Pb end-members and that β -duftite is not a distinct polymorph but rather a calcian duftite. Given the space group assignments of Guillemin (1956) it appeared that there would be a change in symmetry at some point along the duftite-conichalcite compositional join.

Sokolova *et al.*, (1982) reported the crystal structure of duftite in space group $P2_12_12_1$ but were only able to achieve an R factor of 12.2 %. Effenberger and Pertlik (1988), in a conference abstract, reported a refinement of synthetic duftite in space group $P2_12_12_1$ but apparently did not publish full details. The crystal structure of conichalcite was determined by Qurashi and Barnes (1963). In order to establish the relationships between duftite and conichalcite and to clarify the nature of the calcium/lead substitution in this series, and the nature of β -duftite, we undertook a crystal structure refinement of duftite and an examination of ' β -duftite' by powder X-ray diffraction methods and electron diffraction. In this paper we will use the name duftite to represent Guillemin's ' α -duftite' and use ' β -duftite' for the Ca bearing duftite-like mineral where appropriate.

Experimental

A number of duftite and β -duftite specimens from Broken Hill, N.S.W, Mount Bonnie, Northern Territory, and Tsumeb, Namibia, were examined but no crystals suitable for single crystal structure analysis could be found. Attempts were made to synthesize both duftite and β -duftite.

Solutions were prepared following the method of Guillemin (1956). Aqueous solutions of 0.01 M $\text{Cu}(\text{CH}_3\text{CO}_2)_2 \cdot \text{H}_2\text{O}$, 0.01 M $\text{Pb}(\text{CH}_3\text{CO}_2)_2 \cdot 3\text{H}_2\text{O}$ and 0.01 M $\text{Na}_2\text{H}(\text{AsO}_4) \cdot 7\text{H}_2\text{O}$, were mixed and 0.1 M HClO_4 was added to adjust the pH to 3. When the reaction mixture was heated in teflon-lined hydrothermal bombs at 200°C and 15.3 atm for 120 hours well-formed single crystals of duftite of dimensions $0.1 \times 0.05 \times 0.03$ mm

were produced. Similar methods were employed in attempts to synthesize β -duftite; in these experiments between 5 and 30 mol.% of the Pb was replaced by Ca. Calcium was added to the reaction mixture in the form of CaCO_3 . Despite numerous experiments over a 2 year period, where the conditions were systematically varied, β -duftite or calcian duftite could not be synthesized.

Synthetic products and natural samples were identified using powder X-ray diffraction methods. Diffraction patterns were recorded using an 80 mm, Hagg-Guinier camera with monochromated $\text{Cu-K}\alpha_1$ ($\lambda = 1.54051 \text{ \AA}$) radiation, with elemental Si as an internal standard. Preliminary identification was made by referring to the JCPDS powder diffraction file or Guillemin (1956). Subsequently, the patterns were fully indexed and the unit cell parameters of the minerals were refined by least squares methods.

For examination in the transmission electron microscope, crystals or crystal fragments were ground under an organic solvent in an agate mortar and dispersed on Cu grids coated with holey carbon support films. The fragments were examined in a Philips CM200 transmission electron microscope.

Chemical analyses of natural ' β -duftite' were performed using a JEOL electron probe micro-analyser with a wavelength dispersive analysis system, operating under the following conditions: accelerating voltage, 15 kV, beam current, 20 nA, counting time 10 s on the peak, 5 s for the background. The standards employed were: galena (Pb), hematite (Fe), fluorapatite (P), arsenopyrite (As), wollastonite (Ca), sphalerite (Zn, S), Cu metal (Cu).

Refinement of the structure of duftite

Examination of synthetic duftite crystals by petrographic microscope revealed that they were suitable for the single-crystal X-ray analysis; they showed clear and sharp extinction. Precession photographs confirmed orthorhombic symmetry and the systematic absences were $h00, h = 2n + 1$; $0k0, k = 2n + 1$; $00l, l = 2n + 1$, uniquely defining the space group $P2_12_12_1$. A data set was collected on an Enraf-Nonius CAD4 turbo diffractometer at the University of New South Wales. The unit cell dimensions were obtained by a least squares fit of the setting angles for 25 selected and centred reflections. Intensities of 1554 reflections were collected with graphite-monochromatized $\text{Mo-K}\alpha$

radiation ($\lambda = 0.7107 \text{ \AA}$) using a $\theta/2\theta$ scan. Data for the crystal, the intensity data collection and structure refinement are summarized in Table 1. Calculations relating to the structure solution and refinement were done with the XTAL 3.2 program system (Hall *et al.*, 1992). An absorption correction calculated from the crystal shape (Gaussian quadrature) was applied to the data set and the reflections were sorted and merged to average symmetrically equivalent reflections.

Initial attempts to refine the structure starting with the coordinates from Sokolova *et al.*, (1982), were not satisfactory, converging with $R = 0.15$. The heavy atom method was then employed to solve the structure in the space group $P2_12_12_1$ from the intensity data. A Patterson map was calculated to identify the position of the Pb atom. The positions of the next heavy atoms, As and Cu, were then obtained from a difference Fourier and subsequent difference maps revealed the positions of the O atoms.

The positional parameters for the atoms were refined with isotropic displacement parameters; this gave an $R = 0.07$. Further refinement with the displacement parameters for metal atoms allowed to vary anisotropically gave $R = 0.046$.

Description of the structure of duftite

The final atomic coordinates and displacement parameters from the refinement are given in Table 2 and selected interatomic distance and bond angles are provided in Table 3. A summary of the bond valence calculations for the duftite structure is given in Table 4. The final list of observed and calculated structure factor amplitudes is given in Table 5 (deposited with the Editor).

The structure of duftite consists of edge sharing chains of $\text{Cu}(\text{O},\text{OH})_6$ 'octahedra' running parallel to c . The $\text{Cu}(\text{O},\text{OH})_6$ chains are linked by AsO_4 tetrahedra which share three corners with the chains of octahedra and thus form a three-dimensional network. Lead atoms occupy square antiprismatic cavities in the network (Fig. 1).

The 'octahedral' co-ordination of Cu by O and OH shows a characteristic Jahn-Teller distortion around Cu^{2+} . The interatomic distances of the Cu-octahedron fall into two groups: four short equatorial bonds, ranging between 1.92 and 2.13 \AA and two long apical bonds, 2.31 and 2.38 \AA . The elongation of each octahedron lies approximately parallel to $[62\bar{7}]$ and the three symmetrically related directions $[\bar{6}27]$, $[\bar{6}2\bar{7}]$ and

TABLE 1. Crystal data for duftite

Formula	PbCu(AsO ₄)(OH)
Molecular Weight	426.7
Space group	$P2_12_12_1$
$a(\text{\AA})$	7.768(1)
$b(\text{\AA})$	9.211(1)
$c(\text{\AA})$	5.999(1)
$V(\text{\AA}^3)$	429.2
$D_{\text{calc}}(\text{g cm}^{-3})$	6.602
Z	4
$\mu(\text{mm}^{-1})$	51.64
$\lambda(\text{Mo K}\alpha)(\text{\AA})$	0.7101
Crystal dimensions	0.1 × 0.05 × 0.03 mm
$T_{\text{min}}, T_{\text{max}}$	0.006, 0.112
Data Collection:	
Diffractometer	Enraf-Nonius CAD4
Turbo	
$\theta_{\text{max}}(\text{^\circ})$	30
h	-10 → 10
k	0 → 12
l	-8 → 8
Total reflections measured	1554
Number after averaging	680
R for averaging	0.084
Refinement:	
Refinement on	F
Weight	$1/\sigma^2(hkl)$
R	0.046
R_w	0.065
Reflections used in refinement ($F > 2\sigma$)	640
Number of parameters refined	48
H atoms not located	
Goodness of fit S	1.76(5)
$(\Delta\sigma)_{\text{max}}$	0.002
$\Delta q_{\text{max}}, \Delta q_{\text{min}}(\text{e \AA}^{-3})$	-2.66, 3.25

$[62\bar{7}]$, that is at an angle of about 71° away from b towards c . (Fig. 1). Similar Jahn-Teller distortions of Cu co-ordination have been observed in a number of other copper minerals including: malachite, lindgrenite and linarite (Table 6).

In duftite the Pb is coordinated by eight oxygen atoms arranged at the corners of a distorted square antiprism. The range of Pb-O bond lengths is 2.50–2.81 \AA with an average of 2.66 \AA . Within each AsO_4 tetrahedron there are three short and one long As-O bonds.

The bond valence sums (BVS) for O(1) and O(5) are low, being 1.40 and 1.64 valence unit (ν) respectively while those of the other O atoms

TABLE 2. Atomic coordinates and displacement parameters for duftite

	<i>x</i>	<i>y</i>	<i>z</i>			
Pb	0.3764(1)	0.1668(1)	0.4793(2)			
Cu	0.2556(4)	0.4963(4)	0.7537(4)			
As	0.3686(2)	-0.1934(2)	0.5076(4)			
O(1)	0.385(2)	0.438(1)	0.497(3)			
O(2)	0.142(2)	0.285(2)	0.765(3)			
O(3)	0.126(2)	0.305(2)	0.241(3)			
O(4)	0.541(2)	-0.085(2)	0.494(3)			
O(5)	0.197(2)	-0.085(2)	0.538(3)			
	U11	U22	U33	U12	U13	U23
Pb	0.0102(4)	0.0091(4)	0.0142(4)	0.0018(3)	-0.0002(3)	0.0002(3)
Cu	0.014(1)	0.0071(9)	0.002(1)	-0.0006(8)	-0.001(1)	-0.0032(9)
As	0.0078(8)	0.0047(7)	0.007(1)	-0.0004(6)	0.0020(9)	-0.0003(7)
O(1)	0.008(2)					
O(2)	0.017(3)					
O(3)	0.012(3)					
O(4)	0.012(3)					
O(5)	0.020(3)					

TABLE 3. Selected bond lengths and angles for duftite

Pb—O		Cu—O		As—O	
O(1)	2.50(1)	O(1)	1.92(1)	O(2) ⁱⁱ	1.68(2)
O(2)	2.73(2)	O(1) ^{iv}	1.93(1)	O(3) ⁱⁱⁱ	1.74(2)
O(2)i	2.57(2)	O(2)	2.13(2)	O(4)	1.67(1)
O(3)	2.73(2)	O(3)	2.05(2)	O(5)	1.67(2)
O(3)i	2.58(2)	O(4) ^v	2.31(1)		
O(4)	2.65(1)	O(4) ^{vi}	2.38(1)		
O(5)	2.73(2)				
O(5) ⁱⁱ	2.81(2)				

O(5)—As—O(3) 106.50°

O(4)—As—O(5) 106.65°

O(4)—As—O(2) 107.22°

O(5)—As—O(2) 110.71°

O(4)—As—O(3) 111.91°

O(2)—As—O(3) 113.65°

Symmetry — equivalent positions.

(i) $1/2 + x, 1/2 - y, 1 - z$ (ii) $1/2 - x, -y, -1/2 - z$ (iii) $1/2 - x, -y, 1/2 - z$ (iv) $1/2 - x, 1 - y, 1/2 - z$ (v) $1/2 - x, 1/2 + y, 1/2 - z$ (vi) $-1/2 + x, 1/2 - y, 1 - z$

TABLE 4. Summary of bond-valence analysis for duftite

	Pb	Cu	As	SUM
O(1)	0.36	0.52		1.40
O(2)	0.30	0.52	1.25	2.03
	0.19	0.29		
O(3)	0.28	0.37	1.08	1.92
	0.19			
O(4)	0.23	0.18	1.27	1.97
		0.16		
O(5)	0.18		1.30	1.64
	0.16			
SUM	1.89	2.04	4.90	

are close to 2.00 *vu* (see Table 4). Stereochemical and BVS considerations suggest that O(1) is an OH group. It is the only oxygen atom that is coordinated by Pb and two Cu cations but not As and has the lowest BVS. In the PbO_8 polyhedra and CuO_6 octahedra, Pb–O(1) and Cu–O(1) are the shortest metal–oxygen distances. By assuming an average O–H bond length of 0.98 Å for the O(1)–H contact and using the standard r_o value for H bonded to O (0.882) (Brown and Altermatt, 1985) the bond valence contribution is 0.76 *vu* and the sum for O(1) is then 2.16 *vu*. The H bond must then be to O(5), as the second lowest BVS. The O(1)–O(5) distance is 2.80 Å and by assuming linearity of the linkage O(1)–H···O(5) and the O–H bond length 0.98 Å then the O(5)···H contact has a length of 1.82 Å. This would give a bond valence contribution of 0.08 *vu* bringing the bond valence sum for O5 to 1.72 *vu*. This result is consistent with the correlation of O–H···O bonding reported by Brown and Altermatt (1985), however a slightly longer O(1)–H bond length and a shorter H···O(5) contact would give bond valence sums for O(1) and O(5) closer to 2. The position of the H bonding in the structure is shown in Fig. 2.

Comparison of duftite and conichalcite structures

As noted in the introduction duftite is a member of the adelite structural group, and is also related to a number of vanadates including descloizite (Hawthorne and Faggiani, 1979) and cechite (Pertlik, 1989). The descloizite structure, in

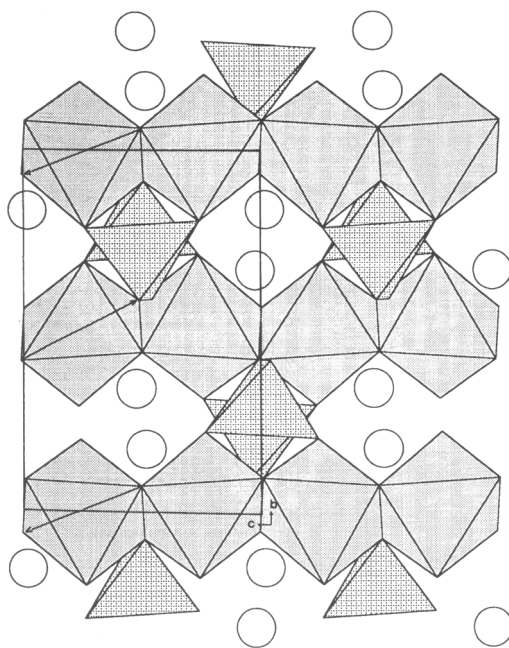


FIG. 1 Schematic diagram of the duftite structure down [100] showing the polyhedral linkages. The Pb atoms are shown as open circles. The arrows indicate the direction of elongation of the CuO_6 octahedra.

space group *Pnam*, can be considered as the archetype or parent structure for the group. In the parent structure all atoms, except one of the O ions occupy special positions on a mirror at $z = 0.25$. The cation distribution in duftite and

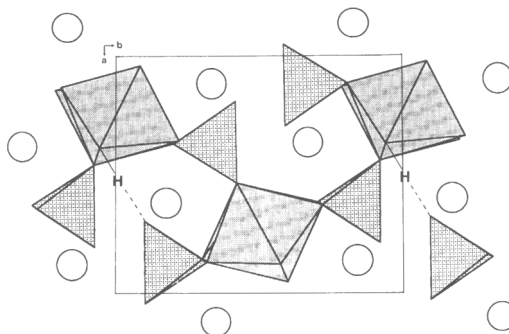


FIG. 2 Schematic diagram of the duftite structure down [001] showing the polyhedral linkages and the proposed hydrogen bonding network. The Pb atoms are shown as open circles.

TABLE 6. Jahn-Teller distorted CuO₆ octahedra in copper oxysalt minerals

Mineral		Equatorial				Apical		Ref
duftite	PbCu(AsO ₄)(OH)	1.92	1.93	2.13	2.05	2.31	2.38	1
conichalcite	CaCu(AsO ₄)(OH)	1.95	1.95	2.04	2.09	2.38	2.28	2
malachite	Cu ₂ (CO ₃)(OH) ₂	2.00	2.05	1.90	1.91	2.51	2.64	3
lindgrenite	Cu ₃ (MoO ₄) ₂ (OH) ₂	1.96	1.93	1.98	2.00	2.30	2.47	4
"	"	1.95	1.95	1.98	1.98	2.42	2.42	
linarite	PbCu(SO ₄)(OH) ₂	1.93	1.93	1.98	1.98	2.54	2.54	5
schmiederite	Pb ₂ Cu ₂ (OH) ₄ (SeO ₃)(SeO ₄)	1.95	1.95	1.97	1.98	2.57	2.63	5

(1) this work; (2) Qurashi and Barnes, 1963; (3) Zigan *et al.*, 1977; (4) Hawthorne and Eby, 1985; (5) Effenberger, 1987

conichalcite closely approximate special positions in *Pnam*, however several of the O ions are significantly displaced from the mirror plane requiring the lowering of symmetry to *P2₁2₁2₁*. Thus duftite can be considered as a displacively modulated superstructure of the *Pnam* parent in which the primary modulation vector $\mathbf{q}^{\text{prim}} = 0$ (see Perez-Mato *et al.*, 1987; Withers, 1989; Pring *et al.*, 1993 for discussion of the nomenclature of modulated structures).

Because β -duftite is compositionally intermediate between duftite and conichalcite a detailed comparison of these two structures is most appropriate. The crystal structure of conichalcite, CaCu(AsO₄)(OH) was reported by Qurashi and Barnes (1963). The space group is *P2₁2₁2₁*, the same as duftite, but the unit cell is slightly smaller $a = 7.393$, $b = 9.220$ $c = 5.830$ Å $V = 397.4$ Å³ (Radcliffe and Simmons, 1971). This difference reflects the difference in the size of Pb and Ca cations. It too can be considered as a displacively modulated superstructure of the *Pnam* parent in which the primary modulation vector $\mathbf{q}^{\text{prim}} = 0$. The oxygen co-ordination around As in conichalcite is more distorted than it is in duftite and the AsO₄ tetrahedra are rotated 10° anti-clockwise about *a*. The Cu co-ordination in both structures shows classic Jahn-Teller distortion. However, there is a distinct difference between the direction of the elongation of the Cu(O,OH)₆ octahedra; in conichalcite it runs along the *b* axis whereas in duftite the octahedra are elongated approximately along $\langle 627 \rangle$.

The co-ordination Ca(O,OH)₈ in conichalcite is very similar to Pb(O,OH)₈ in duftite. However there are substantial shifts in the positions of two of the co-ordinating O atoms in conichalcite; O(3)

is displaced along the *b* axis and O(5) along a direction approximately 25° to the *c* axis. These displacements result in a less distorted co-ordination sphere than the Pb(O,OH)₈ square antiprism.

The nature of β -duftite

Guillemin (1956) identified β -duftite as a distinct polymorph of duftite on a number specimens from Tsumeb, later Jambor *et al.* (1980) suggested that it was merely an intermediate in the solid solution series between duftite and conichalcite.

An apparently well-crystallized specimen of β -duftite from Tsumeb, Namibia, from the Museum of the Institute for Mineralogy and Petrology, University of Hamburg (MinMusHH-83/5), was located. On this specimen the β -duftite appeared to be well formed transparent single crystals up to 0.5 mm in length, however precession photographs revealed that the 'single crystals' were disordered. Electron probe microanalysis of crystals from this specimen showed that the Pb:Ca ratio was 59:41 (Table 7) and the simplified formula, based on 5 oxygen atoms, is (Pb_{0.59}Ca_{0.41})(Cu_{0.89}Zn_{0.11})(AsO₄)(OH). This is somewhat more Ca-rich than the β -duftite analysed from the same locality by Guillemin (1956) (i.e Pb:Ca = 76:24).

The least-squares refinement of the β -duftite powder X-ray diffraction data on the orthorhombic cell gave $a = 7.4870(5)$, $b = 9.4451(5)$, $c = 5.9271(5)$ Å and $V = 419.14$ Å³. Thus *a* and *c* cell repeats of β -duftite are shorter than those of duftite and longer than those of conichalcite; however the *b* cell repeat is significantly longer than those of end-member duftite or conichalcite (Table 8).

TABLE 7. Electron microprobe analyses of β -duftite

Oxide	Range (wt.%)	Average (wt.%)*	Atoms
			As+P = 1
PbO	33.77–38.23	35.68	0.588
CaO	5.41–7.36	6.17	0.405
CuO	20.07–22.16	21.52	0.997
ZnO	2.26–2.93	2.64	0.120
As ₂ O ₅	30.12–31.41	30.82	0.987
P ₂ O ₅	0.14–0.55	0.25	0.013
H ₂ O	not determined		

*Mean of 10 analyses.

There is only a small deviation from a linear trend between the Ca and Pb end members for a - and c -repeats, but a substantial departure in the case of the b -repeats (Fig. 3). Overall, however, the cell volume shows no deviation from a linear trend. The small deviation in a and c may be due to the partial substitution of Zn for Cu in some compositions. There is a substantial deviation in the b -cell repeat; it increases significantly at compositions around the mid point in the series. Jambor *et al.* (1980) noted a similar, though not as pronounced trend in their investigations which they attributed to compositional zoning. Evidence for compositional zoning in the specimen used in the current study was sought by electron probe microanalysis but the grains were found to be homogeneous at the resolution offered by the electron microprobe ($> 1 \mu\text{m}$).

Electron diffraction patterns of β -duftite show evidence of an incommensurately modulated superstructure. Figure 4 shows the [010] and

[100] zone electron diffraction patterns. Note the distribution of intensity in the Bragg reflections. The [100] zone pattern shows $0kl$, $k+l=2n$ while the [010] zone shows $h00$, $h=2n$; $00l$, $l=2n$ and $h0l$, $h=2n$, the set of systematic absences which corresponds to space group $Pnam$ in the setting used here. It was noted above that the cation distribution in duftite and conicalcrite closely approximate special positions in $Pnam$ while the oxygen atoms are displacively modulated, lowering the symmetry to $P2_12_12_1$. In β -duftite the modulation is no longer commensurate. In addition to the Bragg reflections G , superlattice reflections are also present, but they are distributed only around the reflections which are forbidden by the n and a glides in the parent structure. On the [010] zone (Fig. 4a) faint superlattice reflections occur at $h0l$, $h=2n+1$ with a modulation vector $G \pm q^{\text{prim}} \approx 3/13 d_{001}^*$ corresponding to a real space wavelength of $\sim 25.7 \text{ \AA}$. In this case the superlattice reflections are very weak and diffuse. In the [100] zone (Fig. 4b) pairs of superlattice reflections are distributed around the $0kl$, $k+l=2n+1$ reflections with a modulation vector $G \pm q^{\text{prim}} \approx 3/26 d_{001}^*$ which corresponds to a real space wavelength of 51.4 \AA . Here the superlattice reflections are relatively strong and sharp and are in fact slightly canted off [001], the actual direction being close to [013].

The origin of the structural modulation superlattices is a question of some importance. Structural modulations can be either compositional or displacive in origin, and in the case of gross compositional modulation, there is usually an associated displacive component. Withers (1989) suggested that it is possible to distinguish between compositional and displacively modulations on the

TABLE 8. Cell parameters of members of the duftite–conicalcrite series*

Pb:Ca	Cu:Zn	a (Å)	b (Å)	c (Å)	V (Å ³)	Ref
100:0	100:0	7.768	9.211	5.999	429.2	1
100:0	100:0	7.778	9.207	6.000	429.7	2
93:7	96:4	7.716	9.178	5.954	421.6	2
59:41	89:11	7.487	9.445	5.927	419.1	1
41:59	90:10	7.446	9.255	5.881	405.3	2
40:60	89:11	7.461	9.202	5.864	402.6	2
20:80	69:31	7.465	9.185	5.892	404.0	2
0:100	100:0	7.393	9.220	5.830	397.4	3

(1) this work (2) Jambor *et al.* (1980) (3) Radcliffe and Simmons (1971)

* cell data have been reset to a common orientation

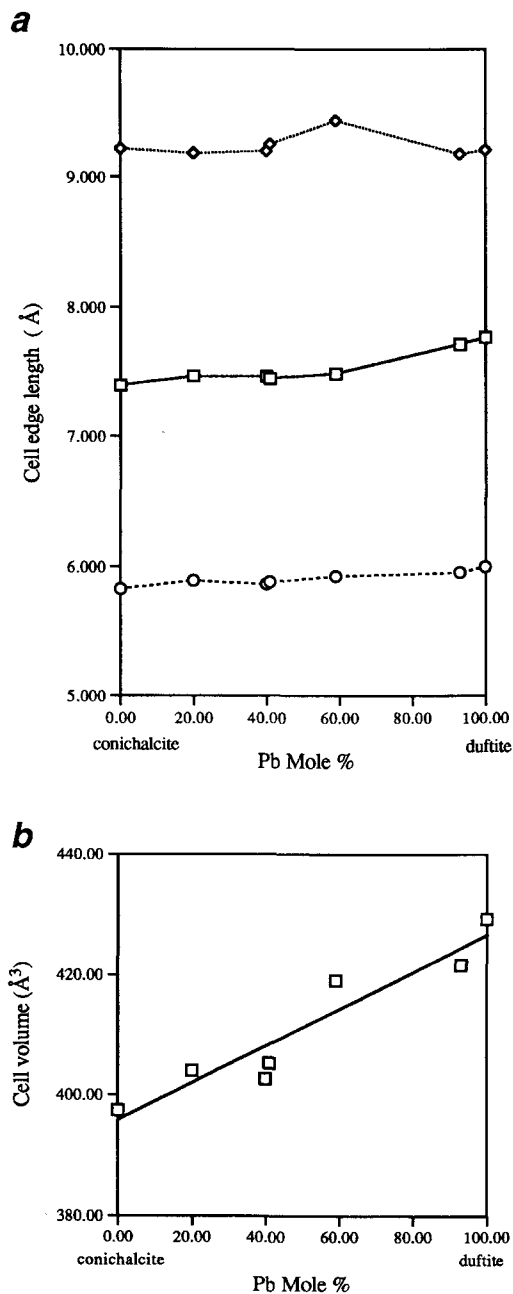


FIG. 3. (a) Comparison of the trends of the three unit cell repeats for members in the duftite-conicalcrite series. (b) plot of composition against cell volume for members of the duftite-conicalcrite series.

basis of the intensity distribution in the superlattice reflections. Thus, in the case of compositional modulation, the satellite reflections are strongest near the centre of the diffraction pattern, whereas for a displacive modulation, the intensity of the satellite reflections initially increase as $|\mathbf{G}^* \pm m\mathbf{q}|$ increases until the contribution of the temperature factor component of intensity dominates, and the intensity decays. The intensity distribution in the satellite reflections in Fig. 4b, the clearer of the diffraction patterns, suggests to us a displacive origin for the modulation.

Unfortunately it is not possible to resolve the nature of the modulated structure in β -duftite unequivocally on the basis of these electron diffraction patterns. However comparison of the structural data suggests a possible origin. The distinct deviation of the *b*-cell, at the mid-member composition, is linked to changes in the orientation of the tetragonal distortion of the CuO_6 octahedron. As noted above, the orientation of the Jahn-Teller elongation of the CuO_6 octahedron in duftite is approximately 71° from the *c* axis whereas in conicalcrite the orientation of the Jahn-Teller distortion is parallel to the *b* axis. This difference in orientation results in a substantial difference in the length of the octahedra parallel to the *b* axis (duftite, 4.18Å; conicalcrite, 4.66Å). The substitution of 41% Ca for Pb in β -duftite results in approximately one half of the chains of octahedra being composed of octahedra with Jahn-Teller elongation of conicalcrite-type and one half with octahedra of duftite-type. The fact that the superlattice reflections occur only about *Pnam* forbidden reflections suggests that the Pb and Ca are not ordered on a supercell. If metal distribution were also modulated one would expect superlattice reflections around reflections with $0kl$, $k+l = 2n$ and $h0l$, $h = 2n$. It seems most likely that the modulation is linked to displacements of the oxygen atoms in β -duftite. The size of the domains could be expected to vary greatly with small changes in composition as they do in the plagioclase feldspars (Putnis, 1992).

Clearly β -duftite is not a distinct mineral but is a composition or a series of compositions in the duftite-conicalcrite series. It is also evident that the duftite-conicalcrite series is not a simple solid solution but is rather more complex. A detailed study of other compositions in the series is required before a detailed understanding of the series can be obtained. It is also clear, given the modulated structure of the β -duftite, why synthesis was not possible.

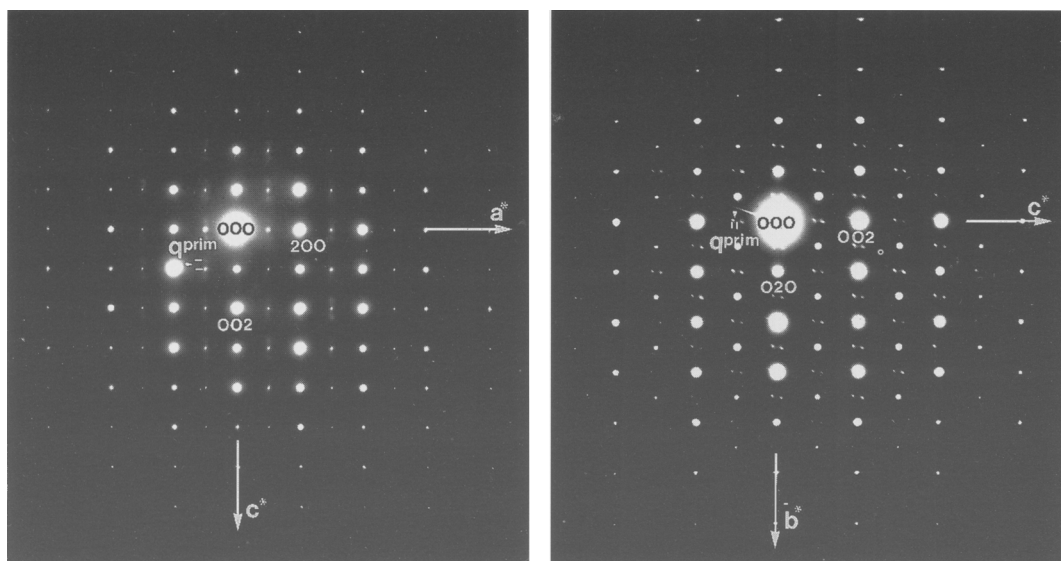


FIG. 4. Electron diffraction patterns of β -duftite showing an apparently incommensurate superlattice. (a, left) The [010] zone with faint superlattice reflections at $h0l$, $h = 2n + 1$ with a modulation vector $\mathbf{G} \pm \mathbf{q}^{\text{prim}} \approx 3/13 \mathbf{d}_{001}^*$. (b, right) The [100] zone showing pairs of superlattice reflections are distributed around the $0kl$, $k + l = 2n + 1$ reflections with a modulation vector $\mathbf{G} \pm \mathbf{q}^{\text{prim}} \approx 3/26 \mathbf{d}_{001}^*$.

Acknowledgements

We wish to thank AusAID for the award of a scholarship to one of us (K) and Mr D. Craig of the University of New South Wales for assistance with the single crystal data collection. Dr Jochum Schluter, Institute of Mineralogy, University of Hamburg supplied the sample of β -duftite and Dr W.D. Birch, Museum of Victoria undertook the electron microprobe analyses. We also would like to thank the anonymous reviewer who pointed out a number of errors in an earlier version of the manuscript.

References

- Brown, I.D. and Altermatt, D. (1985) Bond valence parameters obtained from a systematic analysis of the inorganic crystal structure database. *Acta Crystallogr.*, **B41**, 241–7.
- Effenberger, H. (1987) Crystal structure and chemical formula of schmiederite, $\text{Pb}_2\text{Cu}_2(\text{OH})_4(\text{SeO}_3)(\text{SeO}_4)$, with a comparison to linarite, $\text{PbCu}(\text{OH})_2(\text{SO}_4)$. *Mineral. Petrol.*, **36**, 3–12.
- Effenberger, H. and Pertlik, F. (1988) Comparison of the homeomorphic crystal structures of $\text{Pb}(\text{Fe}, \text{Mn})(\text{VO}_4)(\text{OH})$ = cechite and $\text{PbCu}(\text{AsO}_4)(\text{OH})$ = duftite. *Z. Kristallogr.*, **185**, 610 (abstract).
- Guillemin, C. (1956) Contribution a la minéralogie des arsénates, phosphates et vanadates de cuivre. 1 Arsénates de cuivre. *Bull. Soc. fr. Minéral. Cristallogr.*, **79**, 7–95.
- Hall, S., R., Flack, H.D. and Stewart, J.M. (Eds) (1992). *Xtal3.2 Reference Manual*. University of Western Australia, Perth, Australia.
- Hawthorne, F.C. and Eby, R.K. (1985) Refinement of the crystal structure of lindgrenite. *Neues Jahrb. Mineral. Mh.*, 234–40.
- Hawthorne, F.C. and Faggiani, R. (1979) Refinement of the structure of descloizite. *Acta Crystallogr.*, **B35**, 717–20.
- Jambor, J.L., Owens, D.R. and Dutrizac, J.E. (1980) Solid solution in the adelite group of arsenates. *Canad. Mineral.*, **18**, 191–5.
- Keller, P. (1977) Tsumeb, VI Paragenesis. *Miner. Record*, **8**, 36–47.
- Perez-Mato, G., Madariaga, G., Zuñiga, F.J. and Garcia Arribas, S.A. (1987) On the structure and symmetry of incommensurate Phases. a practical formulation. *Acta Crystallogr.*, **A43**, 216–26.
- Pertlik, F. (1989) The crystal structure of cechite, $\text{Pb}(\text{Fe}^{2+}, \text{Mn}^{2+})(\text{VO}_4)(\text{OH})$ with $\text{Fe} > \text{Mn}$. A mineral

- of the descloizite group. *Neues Jahrb. Mineral. Mh.*, 34–40.
- Pring, A., Williams, T.B. and Withers R.L. (1993) Structural modulation in sartorite: an electron microscope study. *Amer. Mineral.*, **78**, 619–26.
- Pufahl, O. (1920) Mitteilungen über Mineralien und Erze von Südwestafrika, besonders solche von Tsumeb. *Centralblatt für Mineralogie, Geologie, und Paläontologie*, 289–96.
- Putnis A. (1992) *Introduction to Mineral Sciences*. Cambridge University Press, 434–7.
- Qurashi, M. M. and Barnes, W.H. (1963) The structures of the minerals of the descloizite and adelite groups: IV- Descloizite and conicalcrite (Part 2) the structure of conicalcrite. *Canad. Mineral.*, **7**, 561–77.
- Radcliffe, D. and Simmons, W.B. Jr (1971) Austinite: chemistry and physical properties in relation to conicalcrite. *Amer. Mineral.*, **56**, 1359–65.
- Richmond, W.E. (1940) Crystal chemistry of the phosphates, arsenates and vanadates of the type $A_2XO_4(Z)$ *Amer. Mineral.*, **25**, 441–78.
- Sokolova, E.V., Egorov-Tismenko, Y. K. and Yakhonoptova P.K. (1982) Research on crystal structure of rare arsenates: duftite and mimetite *Vest. Mosk Univ. Ser.*, **4**, 50–6 (Russian).
- Taggart, J.E. and Foord, E.E. (1980) Conicalcrite, cuprian austinite, and plumbian conicalcrite from La Plata County, Colorado. *Mineral. Record*, **11**, 37–8.
- Withers, R.L. (1989) The characterization of modulated structures via their diffraction patterns. *Prog. Crystal Growth Character.*, **18**, 139–204.
- Zigan, F., Joswig, W., Schuster, H.D. and Mason, S.A. (1977) Verfeinerung der structure von malachit, $Cu_2(OH)_2CO_3$ durch Neutronenbeugung. *Z. Kristallogr.*, **145**, 412–26.

[Manuscript received 6 January:
revised 27 February 1997]